

Short Communication

Fast and efficient reduction of nitro aromatic compounds over Fe₃O₄/β-alanine-acrylamide-Ni nanocomposite as a new magnetic catalystFarzad Zamani ^{a,b,*}, Sahar Kianpour ^b^a Department of Chemistry, Shahreza Branch, Islamic Azad University, Shahreza 31186145, Isfahan, Iran^b Laboratory of Applied Chemistry, Central Laboratory Complex, Isfahan Science and Technology Town, Isfahan University of Technology, Isfahan 8415683111, Iran

ARTICLE INFO

Article history:

Received 19 September 2013

Received in revised form 20 October 2013

Accepted 22 October 2013

Available online 30 October 2013

Keywords:

Heterogeneous magnetic catalyst

Nickel nanoparticle

β-Alanine

Acrylamide

Reduction reaction

ABSTRACT

In this study, Ni nanoparticles incorporated β-alanine-acrylamide (Ala-AA) was successfully prepared by a simple method. The obtained magnetic nanocomposite exhibited excellent activity as a new heterogeneous magnetic catalyst for the reduction of a number of nitro aromatic compounds under mild conditions along with high level of reusability.

© 2013 Elsevier B.V. All rights reserved.

1. Introduction

Over the last few years, magnetic nanoparticles (e.g. Fe₃O₄) have been extensively investigated as inorganic support for the synthesis of organic–inorganic hybrid materials, due to their potential applications in many industrial and biological fields [1]. Their magnetic character makes them to be effective and easily separated from the reaction media by applying an external magnetic field. In addition, when magnetic nanoparticles are used as supports, the size of the support materials is decreased to the nanometer scale, and all of the catalytic sites on the external surface of the particles can be accessible to the substrates [2]. As a consequence, the activity of these nanoparticle-supported catalysts could be improved compared to conventional heterogeneous catalysts based on porous support matrices, where internal pore diffusion in the porous catalysts can represent a rate limiting step [2]. In this way, organic–inorganic hybrid materials based on magnetic nanoparticles have been widely used in the field of biology, medicine and catalysis [3–6].

In recent years, modified magnetic nanoparticles have received a lot of attention as support for preparation of noble metal nanoparticles [7–22]. However, most of these techniques use organosilica precursors as organic shell in order to prepare a suitable support for trapping metal nanoparticles. The organosilane precursors not only involve complicated synthesis and purification method, but also are very expensive

and toxic. Therefore, from both environmental and economic points of view, preparation of the modified magnetic nanoparticles via a simple method and without using organoalkoxysilane compounds is highly desirable.

The reduction of nitro compounds to amino compounds is industrially important as the amines obtained are commercially important starting materials and intermediates for a number of valuable compounds such as pharmaceuticals, agrochemicals and dyes [23,24]. In this regard, a variety of reducing systems and catalysts has been used for catalytic reduction of nitro compounds [25–33].

In continuing our efforts towards the development of efficient and environmentally benign heterogeneous catalysts [34,35], herein, Fe₃O₄/β-alanine-acrylamide nanocomposite containing Ni nanoparticles was prepared via a simple method without using organosilane precursors, as a novel heterogeneous magnetic catalyst. The catalytic activity of this magnetic nanocomposite was tested in the reduction of different nitro aromatic compounds in the presence of sodium borohydride (NaBH₄) as a mild reducing agent.

2. Experimental

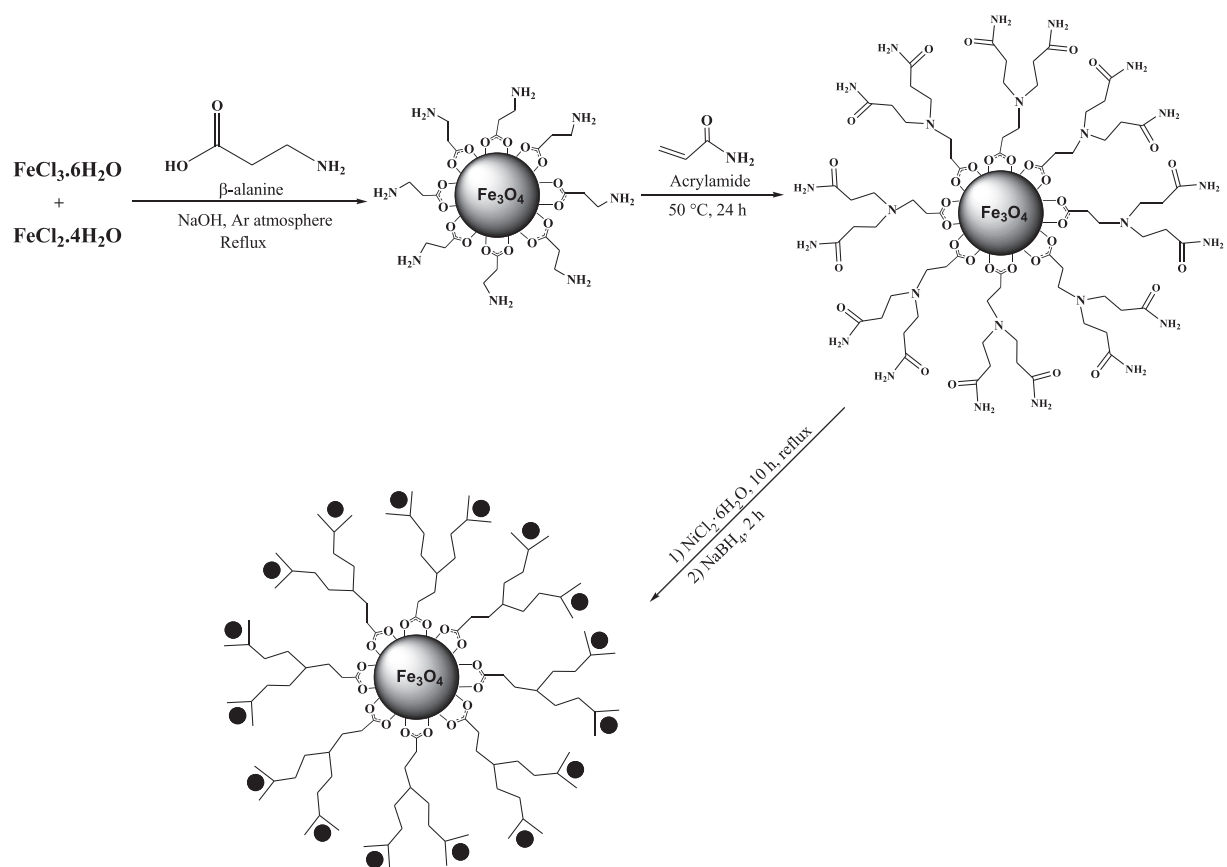
2.1. Catalyst preparation

The procedure for preparing the Fe₃O₄/Ala-AA-Ni nanocomposite includes three steps. The overall schematic procedure used to synthesize the magnetic catalyst was illustrated in Scheme 1, and the detailed procedure was described as follows.

In the first step, magnetic nanoparticles were prepared in the presence of β-alanine amino acid via a simple co-precipitation route reported

* Corresponding author at: Department of Chemistry, Shahreza Branch, Islamic Azad University, Shahreza 31186145, Isfahan, Iran. Tel.: +98 311 3865355; fax: +98 311 3869714.

E-mail address: fzamani@iaush.ac.ir (F. Zamani).



Scheme 1. Schematic representation procedure for the preparation of $\text{Fe}_3\text{O}_4/\text{Ala-AA-Ni}$ nanocomposite.

in an early study [36]. $\text{FeCl}_3 \cdot 6\text{H}_2\text{O}$ (13 g, 0.048 mol), $\text{FeCl}_2 \cdot 4\text{H}_2\text{O}$ (4.8 g, 0.024 mol) and β -alanine (8.5 g, 0.096 mol) were dissolved in 100 mL deionized water. Then, the solution pH was adjusted to 11 with NaOH solution (2 M) to form a black suspension. Afterwards, the suspension was reflux for 12 h under vigorous stirring and Ar atmosphere. Finally, the obtained nanocomposite was separated from the aqueous solution by magnetic decantation, washed several times with deionized water and dried in an oven overnight to yield $\text{Fe}_3\text{O}_4/\text{Ala}$.

In the second step, Michael addition of acrylamide (AA) to amino groups on the surface of Fe_3O_4 nanoparticles was carried out as the following. At first, 0.5 g of $\text{Fe}_3\text{O}_4/\text{Ala}$, 7 mL of methanol and acrylamide (1 g, 0.014 mol) were placed in a round bottom flask. Then, the mixture was stirred at 50 °C for 24 h. Finally, the resulting powder ($\text{Fe}_3\text{O}_4/\text{Ala-AA}$) was separated by an external magnet, washed several times with methanol and dried at room temperature.

In the last step, incorporation of nickel nanoparticles onto the $\text{Fe}_3\text{O}_4/\text{Ala-AA}$ nanocomposite was carried out by mixing the $\text{Fe}_3\text{O}_4/\text{Ala-AA}$ (1 g) and $\text{NiCl}_2 \cdot 6\text{H}_2\text{O}$ (0.12 g) in methanol (30 mL) and was refluxed for 10 h. Then, the reaction was cooled at room temperature and NaBH_4 solution (catalyst: $\text{NaBH}_4 = 1:5$) was added dropwise to the mixture and stirred for 2 h. Finally, the synthesized nanocomposite ($\text{Fe}_3\text{O}_4/\text{Ala-AA-Ni}$) was separated from the suspension by magnetic decantation, washed several times with deionized water and methanol, and dried under vacuum at room temperature. The weight percentage of Ni in the $\text{Fe}_3\text{O}_4/\text{Ala-AA-Ni}$, as determined by inductively coupled plasma (ICP), was 6.12 wt.%.

2.2. General procedure for the reduction of nitro aromatic compounds

In a typical procedure, a mixture of nitrobenzene (2 mmol), NaBH_4 (6 mmol), $\text{Fe}_3\text{O}_4/\text{Ala-AA-Ni}$ (0.03 g) and water (3 mL) was placed in a round bottom flask. The suspension was stirred at room temperature.

The reaction process was monitored by thin layer chromatography (TLC). At the end of the reaction, the residue was extracted with diethyl ether. The organic layer was dried over Na_2SO_4 and the solvent was removed under reduced pressure. Pure product was obtained by column chromatography over silica gel using hexane/ethyl acetate as eluent. The products were identified with ^1H NMR, ^{13}C NMR and FT-IR spectroscopy techniques.

3. Results and discussion

Crystalline structures of the $\text{Fe}_3\text{O}_4/\text{Ala-AA}$ and $\text{Fe}_3\text{O}_4/\text{Ala-AA-Ni}$ were analyzed by XRD (Fig. 1a, b) (evaluated by Bruker D8 Advance diffractometer). According to Fig. 1, the diffraction peaks corresponding to the Fe_3O_4 crystals [37] are observable in both samples. Furthermore, apart from the original peaks related to Fe_3O_4 , the new diffraction peaks of the (111) and (200) planes of *fcc* nickel nanoparticle [38] are present in the spectrum of $\text{Fe}_3\text{O}_4/\text{Ala-AA-Ni}$ which indicate the existence of Ni element in the form of Ni(0) (Fig. 1b), although characteristic diffraction peak of (111) overlapped with that of Fe_3O_4 nanoparticles.

The FT-IR spectra of $\text{Fe}_3\text{O}_4/\text{Ala}$, $\text{Fe}_3\text{O}_4/\text{Ala-AA}$ and $\text{Fe}_3\text{O}_4/\text{Ala-AA-Ni}$ nanocomposites were recorded to confirm the modification of the magnetite surface with the organic shell and Ni nanoparticles (Fig. 2a–c) (recorded with PerkinElmer 65 spectrometer). The presence of magnetite nanoparticles is observable by the strong adsorption band at 589 cm^{-1} , corresponding to the Fe–O vibrations (Fig. 2a–c). In the case of $\text{Fe}_3\text{O}_4/\text{Ala}$ (Fig. 2a), the adsorption peaks at 1447, 1589, 1416 and 3244 cm^{-1} are due to bending vibration of N–H, asymmetric and symmetric stretching of COO^- , and stretching of N–H, respectively, which indicate the presence of bound β -alanine on the surface of magnetite nanoparticle. Furthermore, it has been reported that the wavenumber separation between the COO^-_{as} and COO^-_{s} IR bands can be used to distinguish the type of the interaction

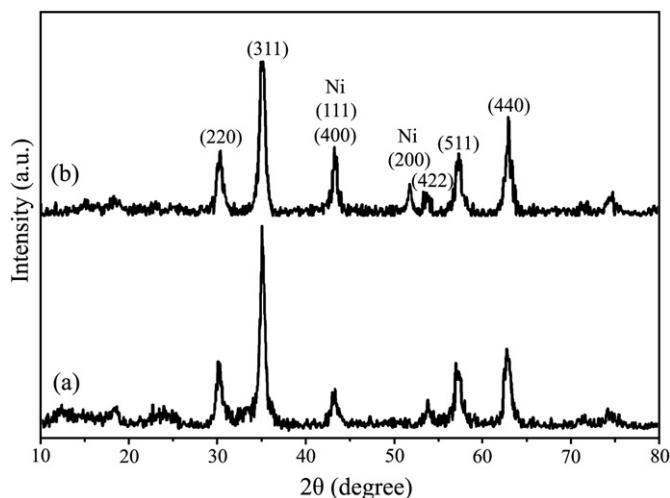


Fig. 1. XRD patterns of (a) $\text{Fe}_3\text{O}_4/\text{Ala-AA}$ and (b) $\text{Fe}_3\text{O}_4/\text{Ala-AA-Ni}$.

between the carboxylate head and the metal atom [39]. Since the wavenumber separation between the COO^-_{as} and COO^-_{s} bands is 173 cm^{-1} ($1589 - 1416 = 173\text{ cm}^{-1}$), it can be concluded that the interaction between the COO^- group and the Fe atom is covalent and bridging bidentate [39]. The presence of peak at around $2800\text{--}3000\text{ cm}^{-1}$ also corresponds to the aliphatic C–H stretching of the methylene groups, which is observable in the samples (Fig. 2a–c). In $\text{Fe}_3\text{O}_4/\text{Ala-AA}$ (Fig. 2b), the new band at 1668 cm^{-1} is due to stretching vibration of C=O bond, indicating the presence of amide group in the nanocomposite. $\text{Fe}_3\text{O}_4/\text{Ala-AA-Ni}$ spectrum (Fig. 2c) shows that the bending vibration absorption band of N–H at 1447 cm^{-1} is shifted to the lower wavenumbers ($1447 \rightarrow 1382\text{ cm}^{-1}$), which is possibly due to the strong interaction between the N groups of amide and metal particles. Moreover, the band at around 1668 cm^{-1} , which is related to the carbonyl bond of AA, is also shifted to the lower wavenumbers ($1668 \rightarrow 1631\text{ cm}^{-1}$). Furthermore, the peak intensity of the carbonyl bond in the spectrum of $\text{Fe}_3\text{O}_4/\text{Ala-AA-Ni}$ is lower than that of $\text{Fe}_3\text{O}_4/\text{Ala-AA}$. These observations may be due to the strong interaction between the Ni nanoparticles and C=O groups. In other words, the double bond CO stretches become weak by coordinating with the metal nanoparticles [40–42], which is confirmed that Ala-

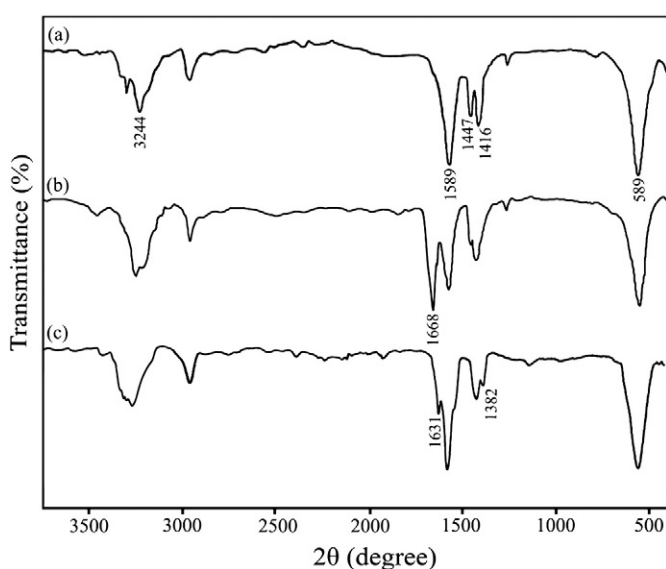


Fig. 2. FT-IR spectra of (a) $\text{Fe}_3\text{O}_4/\text{Ala}$, (b) $\text{Fe}_3\text{O}_4/\text{Ala-AA}$ and (c) $\text{Fe}_3\text{O}_4/\text{Ala-AA-Ni}$.

AA molecules exist on the surface of the nanocomposite, and coordinate with the Ni nanoparticles.

In order to investigate about the state of Ni in the nanocomposite, the XPS study was carried out on the $\text{Fe}_3\text{O}_4/\text{Ala-AA-Ni}$ catalyst (Fig. 3) (recorded with Shimadzu ESCA SSX-100). The Ni 2p spectrum exhibits two main peaks at 851.8 and 868.9 eV which are attributed to Ni(0) $2p_{3/2}$ and Ni(0) $2p_{1/2}$, respectively (Fig. 3). It means that the Ni species are stable as metallic state in the $\text{Fe}_3\text{O}_4/\text{Ala-AA-Ni}$ nanocomposite. Furthermore, it can be seen that the Ni(0) $2p_{3/2}$ and $2p_{1/2}$ binding energy of 851.8 and 868.9 eV represented in Fig. 3 are slightly lower than those of typical Ni nanoparticles (852.3 eV for Ni $2p_{3/2}$ and 869.7 eV for Ni $2p_{1/2}$ [41]). This may be due to the interaction between N and O atoms of Ala-AA and Ni nanoparticles which causes to increase in the charge density around Ni(0) and decrease in binding energy. In general, the binding energy of metal nanoparticles is sensitive to the surrounding chemical environment which means that when the metal species are interacted with ligands, the binding energy will decrease slightly [43]. According to the XPS and IR results, it can be concluded that the Ni nanoparticles were successfully incorporated onto the $\text{Fe}_3\text{O}_4/\text{Ala-AA}$ nanocomposite.

The morphology of the nanocomposite was observed on transmission electron microscopy (performed on Phillips CM10 microscope). Fig. 4 shows TEM image of the $\text{Fe}_3\text{O}_4/\text{Ala-AA-Ni}$ nanocomposite catalyst. As can be seen, the Ni nanoparticles were found to be highly dispersed on the surface of the $\text{Fe}_3\text{O}_4/\text{Ala-AA}$ nanocomposite with the average diameter size of $\sim 3\text{--}4\text{ nm}$.

Fig. 5 depicts the N_2 adsorption–desorption isotherms of the $\text{Fe}_3\text{O}_4/\text{Ala-AA}$ and $\text{Fe}_3\text{O}_4/\text{Ala-AA-Ni}$ nanocomposites (Fig. 5a,b) (recorded with Series BELSORP 18). As can be seen, these isotherms are similar to isotherms of type IV, according to the IUPAC nomenclature, which are the typical characteristics of mesoporous structure [44]. The BET surface areas of the $\text{Fe}_3\text{O}_4/\text{Ala-AA}$ and $\text{Fe}_3\text{O}_4/\text{Ala-AA-Ni}$ nanocomposites were calculated to be $133.7\text{ m}^2\text{ g}^{-1}$ and $96.4\text{ m}^2\text{ g}^{-1}$ respectively. This reduction in the specific surface area may be due to the incorporation of Ni nanoparticles onto the $\text{Fe}_3\text{O}_4/\text{Ala-AA}$ magnetic support.

The structural composition of the $\text{Fe}_3\text{O}_4/\text{Ala-AA-Ni}$ nanocomposite was further examined by energy-dispersive X-ray (EDX) analysis (recorded with Phillips CM10 microscope which was equipped with an energy-dispersive X-ray analyzer). A typical EDX spectrum taken from the nanocomposite was shown in Fig. 6, where peaks associated with Fe, C, O, N, and Ni can be distinguished. The quantitative analysis gives weight ratios of C (39.87%), Fe (20.96%), O (27.62%), N (3.17%) and Ni (6.07%). Taking the EDX analysis into consideration, the presence of Ala-AA-Ni in the structure of magnetic nanocomposite can be further confirmed.

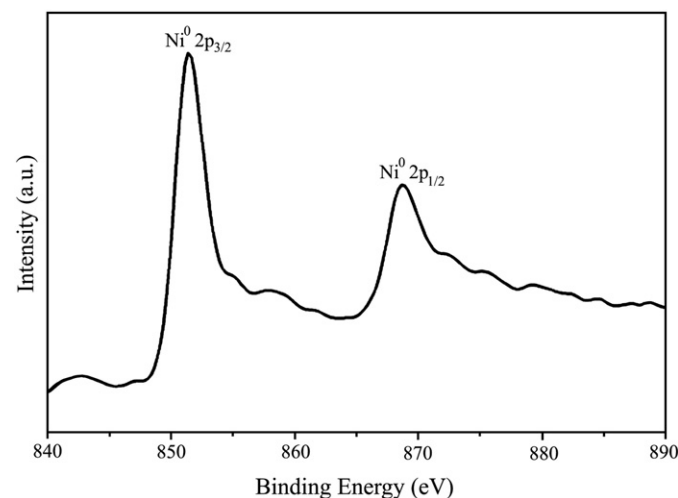


Fig. 3. XPS spectrum of Ni 2p of $\text{Fe}_3\text{O}_4/\text{Ala-AA-Ni}$ nanocomposite.

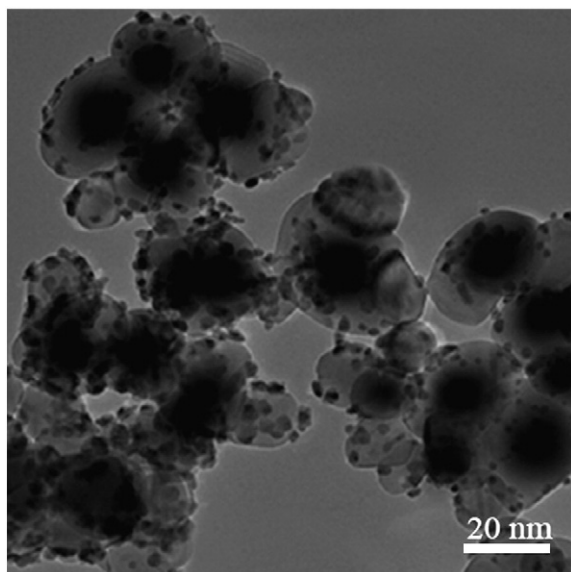


Fig. 4. TEM image of $\text{Fe}_3\text{O}_4/\text{Ala-AA-Ni}$ nanocomposite.

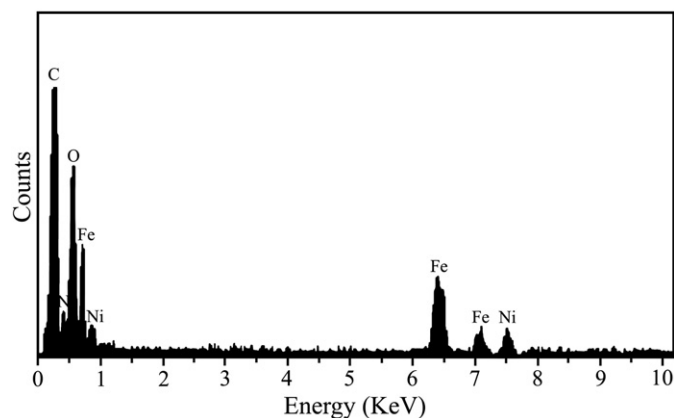


Fig. 6. EDX spectrum of $\text{Fe}_3\text{O}_4/\text{Ala-AA-Ni}$ nanocomposite.

In order to optimize the reaction conditions and to obtain the best catalytic activity, the reduction of nitrobenzene was chosen as a model reaction. The reactions were conducted in water as solvent at room temperature.

The effect of NaBH_4 amount on the reduction reaction was investigated using 0.02 g of the catalyst and 2 mmol of nitrobenzene. The results represented that by increasing the amount of NaBH_4 from 4 mmol to 6 mmol, the yield of the reaction raised significantly from 60% to 79%, while with further increase of the NaBH_4 amount, the yield remained constant. Therefore, 6 mmol of NaBH_4 was chosen as the optimum amount of reducing agent for the further steps.

The reduction reaction of nitrobenzene with NaBH_4 over different amounts of the $\text{Fe}_3\text{O}_4/\text{Ala-AA-Ni}$ was also investigated. It was observed that while the amount of catalyst increased from 0 to 0.03 g, the product yield raised significantly from 0% to 98%, which was probably due to the availability of more active sites (Ni nanoparticles). Since then, the product yield remained stable between 0.03 g and 0.04 g. No reaction yield without using the catalyst corroborates that the $\text{Fe}_3\text{O}_4/\text{Ala-AA-Ni}$ catalyst plays a pivotal role in the reduction of nitro aromatic compounds.

In the view of industrial purposes, reusability of the catalyst was tested by carrying out repeated runs of the reaction on the same batch of the catalyst in the case of the model reaction (Table 1). In order to regenerate the catalyst, after each cycle, it was separated by a magnet, washed several times with deionized water and diethyl ether. Then, it was dried in oven at 60 °C and reused in the subsequent run. According to the results, the $\text{Fe}_3\text{O}_4/\text{Ala-AA-Ni}$ can be reused seven times without

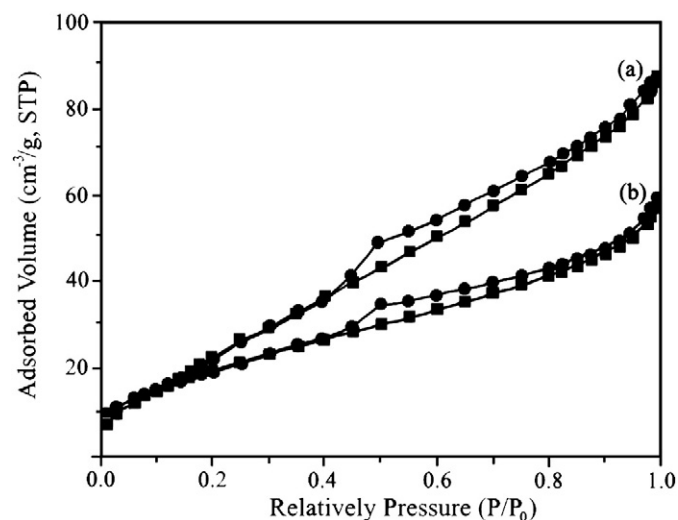


Fig. 5. N_2 adsorption–desorption isotherms of (a) $\text{Fe}_3\text{O}_4/\text{Ala-AA}$ and (b) $\text{Fe}_3\text{O}_4/\text{Ala-AA-Ni}$ nanocomposites.

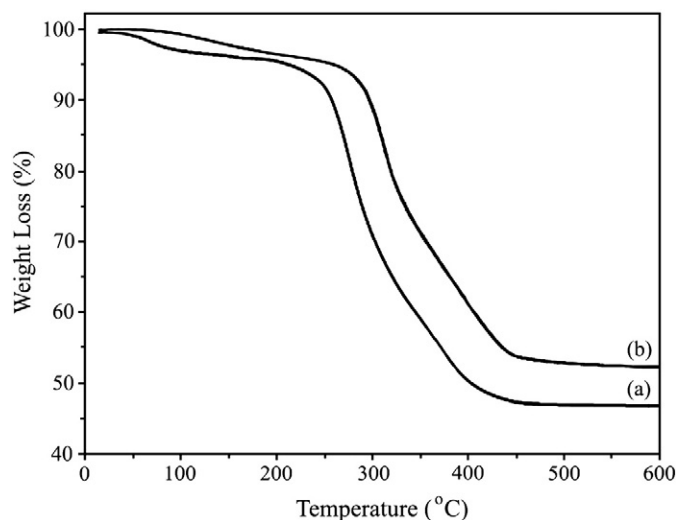


Fig. 7. TG curves of (a) $\text{Fe}_3\text{O}_4/\text{Ala-AA}$ and (b) $\text{Fe}_3\text{O}_4/\text{Ala-AA-Ni}$ nanocomposites.

The thermal stability of the magnetic catalyst before and after modification with Ni nanoparticles was investigated under N_2 atmosphere by thermogravimetric analysis (TGA) (performed on TSTA Type 503). TGA curves of the $\text{Fe}_3\text{O}_4/\text{Ala-AA}$ and $\text{Fe}_3\text{O}_4/\text{Ala-AA-Ni}$ nanocomposites were shown in Fig. 7. It is clearly observed that there are two main weight loss steps in both TG curves. The first one occurs at <150 °C which is due to the desorption of physically adsorbed water in the samples (Fig. 7a, b). In the case of $\text{Fe}_3\text{O}_4/\text{Ala-AA}$, the second step which appears at around 250 °C is related to the decomposition of coating organic layer (Ala-AA) in the nanocomposite (Fig. 7a). However, it can be seen that the $\text{Fe}_3\text{O}_4/\text{Ala-AA-Ni}$ has higher thermal stability than $\text{Fe}_3\text{O}_4/\text{Ala-AA}$ (Fig. 7b, the second step begins at about 300 °C), which may be attributed to the presence of Ni nanoparticles in the nanocomposite structure [45]. Thus, the TGA curves confirm the successful grafting of Ala-AA-Ni onto the surface of magnetic nanoparticles. In addition, comparing the two curves demonstrates that the weight percentage of nickel in the synthesized catalyst is about 6%, which is in agreement with ICP and EDX analysis.

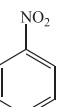
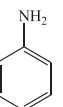
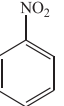
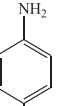
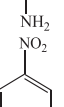
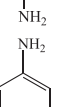
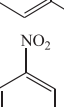
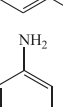
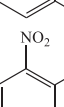
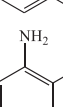
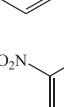
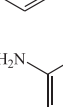
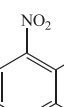
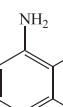
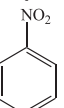
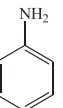
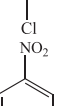
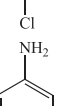
Table 1
The catalyst reusability for the reduction of nitrobenzene.

| Cycle | Yield (%) ^a |
|-------|------------------------|
| Fresh | 98 |
| 1 | 98 |
| 2 | 98 |
| 3 | 96 |
| 4 | 96 |
| 5 | 95 |
| 6 | 93 |
| 7 | 92 |

Reaction conditions: nitrobenzene (2 mmol), Fe₃O₄/Ala-AA-Ni (0.03 g), H₂O (3 mL), NaBH₄ (6 mmol), room temperature, reaction time = 5 min.

^a Isolated yield.

Table 2
Reduction of various nitro aromatic compounds over Fe₃O₄/Ala-AA-Ni.

| Entry | Substrate | Product | Time (min) | Yield (%) ^a |
|-------|---|---|-------------|------------------------|
| 1 |  |  | 5 | 98 |
| 2 |  |  | Immediately | 98 |
| 3 |  |  | Immediately | 98 |
| 4 |  |  | Immediately | 98 |
| 5 |  |  | Immediately | 98 |
| 6 |  |  | 15 | 95 |
| 7 |  |  | 5 | 97 |
| 8 |  |  | 5 | 90 |
| 9 |  |  | 5 | 90 |

Reaction conditions: substrate (2 mmol), Fe₃O₄/Ala-AA-Ni (0.03 g), NaBH₄ (6 mmol), H₂O (3 mL), room temperature.

^a Isolated yield.

any significant loss of activity performance in the reduction of nitrobenzene (decreased by 6%).

In order to prove the heterogeneous nature of the catalyst and to determine the leaching of Ni nanoparticles, heterogeneity test was performed for the optimized reduction reaction of nitrobenzene, in which the catalyst was separated from the reaction mixture at approximately 50% conversion of the starting material. Afterwards, the reaction progress in the filtrate was monitored. No further reduction reaction occurred even at extended times, indicating that the nature of reaction process is heterogeneous and there is not any reaction progress in homogeneous phase. In addition, the reaction solution contained no significant amounts of Ni nanoparticles so that the metal nanoparticles immobilized onto the magnetic support are responsible for the substrate reduction.

The Fe₃O₄/Ala-AA-Ni catalyst also represented high activity in the reduction of different nitro aromatic compounds (Table 2), after ascertaining the optimum experimental conditions. In all cases, the reduction reactions proceed to give the corresponding aniline derivatives in excellent yields and short reaction times.

4. Conclusion

Fe₃O₄ nanoparticles were coated by β-alanine-acrylamide (Ala-AA) organic shell via a simple method, without using any expensive organosilane or bridged organosilane compounds. The Fe₃O₄/Ala-AA nanocomposite was effectively employed as scaffold for in situ generation of Ni nanoparticles. The Fe₃O₄/Ala-AA-Ni nanocomposite was found to be a highly efficient and reusable catalyst in the reduction of various nitro aromatic compounds by NaBH₄ in short reaction times and high yields. These unique results open new perspectives for application of these types of heterogeneous magnetic nanocomposites in other organic reactions.

Acknowledgments

The authors thank the Isfahan Science and Technology Town (Isfahan University of Technology) for the support of this work. The authors also appreciate Dr. A.H. Fani and Dr. M. Ezhe for their helps in the BET and EDX studies.

References

- [1] K.S. Kumar, V.B. Kumar, P. Paik, J. Nanopart. 2013 (2013) 24(Article ID 672059).
- [2] N.T.S. Phan, C.W. Jones, J. Mol. Catal. A Chem. 253 (2006) 123–131.
- [3] G. Liu, R.Y. Hong, L. Guo, Y.G. Li, H.Z. Li, Appl. Surf. Sci. 257 (2011) 6711–6717.
- [4] X.Q. Liu, Y.P. Guan, Z.Y. Ma, H.Z. Liu, Langmuir 20 (2004) 10278–10282.
- [5] A. Kara, B. Erdem, J. Mol. Catal. A Chem. 349 (2011) 42–47.
- [6] M. Kawashita, M. Tanaka, T. Kokubo, Y. Inoue, T. Yao, S. Hamada, T. Shinjo, Biomaterials 26 (2005) 2231–2238.
- [7] B. Sahoo, S.K. Sahu, D. Bhattacharya, D. Dhara, P. Pramanika, Colloids Surf. B Biointerfaces 101 (2013) 280–289.
- [8] W. Li, B. Zhang, X. Li, H. Zhang, Q. Zhang, Appl. Catal. A Gen. 459 (2013) 65–72.
- [9] E. Karagöglü, M.M. Summak, A. Baykal, H. Sozeri, M.S. Toprak, J. Inorg. Organomet. Mater. 23 (2013) 409–417.
- [10] D.C. Li, Z.L. Zhang, S.L. Zhang, Adv. Mater. Res. 177 (2011) 415–417.
- [11] L.M. Rossi, F.P. Silva, L.L.R. Vono, P.K. Kiyohara, E.L. Duarte, R. Itri, R. Landers, G. Machado, Green Chem. 9 (2007) 379–385.
- [12] S. Luo, X. Zheng, J.P. Cheng, Chem. Commun. (2008) 5719–5721.
- [13] K.K. Senapati, S. Roy, C. Borgohain, P. Phukan, J. Mol. Catal. A Chem. 352 (2012) 128–134.
- [14] V. Polshettiwar, B. Baruwati, R.S. Varma, Green Chem. 11 (2009) 127–131.
- [15] C. Borgohain, K.K. Senapati, K.C. Sarma, P. Phukan, J. Mol. Catal. A Chem. 363–364 (2012) 495–500.
- [16] S. He, W. Shi, X. Zhang, J. Li, Y. Huang, Talanta 82 (2010) 377–383.
- [17] S. Wei, Z. Dong, Z. Ma, J. Sun, J. Ma, Catal. Commun. 30 (2013) 40–44.
- [18] K.K. Senapati, C. Borgohain, K.C. Sarma, P. Phukan, J. Mol. Catal. A Chem. 346 (2011) 111–116.
- [19] A. Pourjavadi, S.H. Hosseini, M. Doulabi, S.M. Fakoorpoor, F. Seidi, ACS Catal. 2 (2012) 1259–1266.
- [20] J. Zheng, S. Lin, B.W. Jiang, T.B. Marder, Z. Yang, Can. J. Chem. 90 (2012) 138–144.
- [21] M. Shokouhimehr, J.E. Lee, S.L. Hana, T. Hyeon, Chem. Commun. 49 (2013) 4779–4781.
- [22] A.A. Vernekar, S. Patil, C. Bhata, S.G. Tilve, RSC Adv. 3 (2013) 13243–13250.
- [23] M. Thakur, A. Thakur, K. Balasubramanian, J. Chem. Inf. Model. 46 (2006) 103–110.

- [24] A. Rahman, S.B. Jonnalagadda, *Catal. Lett.* 123 (2008) 264–268.
- [25] Y. Zheng, K. Ma, H. Wang, X. Sun, J. Jiang, C. Wang, R. Li, J. Ma, *Catal. Lett.* 124 (2008) 268–276.
- [26] S. Farhadi, F. Siadatnasab, *J. Mol. Catal. A Chem.* 339 (2011) 108–116.
- [27] S.U. Nandanwar, M. Chakraborty, *Chin. J. Catal.* 33 (2012) 1532–1541.
- [28] F. Wu, L. Qiu, F. Ke, X. Jiang, *Inorg. Chem. Commun.* 32 (2013) 5–8.
- [29] R.J. Kalbasi, A.A. Nourbakhsh, F. Babaknezhad, *Catal. Commun.* 12 (2011) 955–960.
- [30] H. Wen, K. Yao, Y. Zhang, Z. Zhou, A. Kirschning, *Catal. Commun.* 10 (2009) 1207–1211.
- [31] S.K. Ghosh, M. Mandal, S. Kundu, S. Nath, T. Pal, *Appl. Catal. A Gen.* 268 (2004) 61–66.
- [32] E. Kuo, S. Srivastava, C.K. Cheung, W.J. Le Noble, *Synth. Commun.* 15 (1985) 599–602.
- [33] F. Yuste, M. Saldaña, F. Walls, *Tetrahedron Lett.* 23 (1982) 147–148.
- [34] F. Zamani, M. Rezapour, S. Kianpour, *Bull. Korean Chem. Soc.* 34 (2013) 2367–2374.
- [35] F. Zamani, E. Izadi, *Catal. Commun.* 42 (2013) 104–108.
- [36] B. Unal, M.S. Toprak, Z. Durmus, H. Sözeri, A. Baykal, *J. Nanopart. Res.* 12 (2010) 3039–3048.
- [37] L. Cabrera, S. Gutierrez, M.P. Morales, N. Menendez, P. Herrasti, *J. Magn. Magn. Mater.* 321 (2009) 2115–2120.
- [38] D.H. Chen, C.H. Hsieh, *J. Mater. Chem.* 12 (2002) 2412–2415.
- [39] L. Zhang, R. He, H.C. Gu, *Appl. Surf. Sci.* 253 (2006) 2611–2617.
- [40] T. Iwamoto, K. Matsumoto, T. Matsushita, M. Inokuchi, N. Toshima, *J. Colloid Interface Sci.* 336 (2009) 879–888.
- [41] O. Metin, S. Ozkar, *J. Mol. Catal. A Chem.* 295 (2008) 39–46.
- [42] H. Hirai, H. Chawanya, N. Toshima, *React. Polym.* 3 (1985) 127–141.
- [43] H. Li, Z. Zheng, M. Cao, R. Cao, *Microporous Mesoporous Mater.* 136 (2010) 42–49.
- [44] M. Kruk, M. Jaroniec, *Chem. Mater.* 13 (2001) 3169–3183.
- [45] R.J. Kalbasi, N. Mosaddegh, A. Abbaspourrad, *Appl. Catal. A Gen.* 423–424 (2012) 78–90.